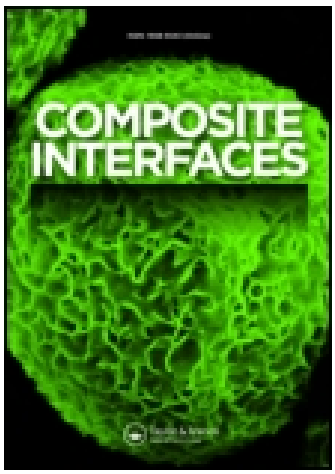
This article was downloaded by: [The University of British Columbia]
On: 10 December 2014, At: 11:08
Publisher: Taylor & Francis
Informa Ltd Registered in England and Wales Registered Number: 1072954 Registered office: Mortimer House, 37-41 Mortimer Street, London W1T 3JH, UK



Composite Interfaces
Publication details, including instructions for authors and subscription information:
http://www.tandfonline.com/loi/tcoi20

Film formation from PS latex doped PNIPAM hydrogels at various heating and cooling rates

Ş. Uğur [a], Ö. Yargi [b] & Ö. Pekcan [c]
[a] Istanbul Technical University, Department of Physics, 34469 Maslak, Istanbul, Turkey
[b] Istanbul Technical University, Department of Physics, 34469 Maslak, Istanbul, Turkey
[c] Isik University, Department of Physics, ¸Sile, 34980 Istanbul, Turkey;, Email: pekcan@isikun.edu.tr
Published online: 02 Apr 2012.

To cite this article: Ş. Uğur , Ö. Yargi & Ö. Pekcan (2008) Film formation from PS latex doped PNIPAM hydrogels at various heating and cooling rates, Composite Interfaces, 15:4, 411-424, DOI: 10.1163/156855408784514748

To link to this article: http://dx.doi.org/10.1163/156855408784514748

PLEASE SCROLL DOWN FOR ARTICLE

Taylor & Francis makes every effort to ensure the accuracy of all the information (the "Content") contained in the publications on our platform. However, Taylor & Francis, our agents, and our licensors make no representations or warranties whatsoever as to the accuracy, completeness, or suitability for any purpose of the Content. Any opinions and views expressed in this publication are the opinions and views of the authors, and are not the views of or endorsed by Taylor & Francis. The accuracy of the Content should not be relied upon and should be independently verified with primary sources of information. Taylor and Francis shall not be liable for any losses, actions, claims, proceedings, demands, costs, expenses, damages, and other liabilities whatsoever or howsoever caused arising directly or indirectly in connection with, in relation to or arising out of the use of the Content.

This article may be used for research, teaching, and private study purposes. Any substantial or systematic reproduction, redistribution, reselling, loan, sub-licensing, systematic supply, or distribution in any form to anyone is expressly forbidden. Terms & Conditions of access and use can be found at http://www.tandfonline.com/page/terms-and-conditions

Composite Interfaces, Vol. 15, No. 4, pp. 411–424 (2008)
© Koninklijke Brill NV, Leiden, 2008.
Also available online - www.brill.nl/ci

Downloaded by [The University of British Columbia] at 11:08 10 December 2014

Film formation from PS latex doped PNIPAM hydrogels at various heating and cooling rates

Ş. UĞUR [1], Ö. YARGI [1] and Ö. PEKCAN [2,*]

[1] *Istanbul Technical University, Department of Physics, 34469 Maslak, Istanbul, Turkey*
[2] *Isik University, Department of Physics, Şile, 34980 Istanbul, Turkey*

Received 6 June 2007; accepted 18 July 2007

Abstract—Film formation from polystrene (PS) latex doped poly(*N*-isopropylacrylamide) (PNIPAM) hydrogels was studied by using photon transmission technique. The transmitted light intensity, I_{tr} was monitored during film formation process. Films were prepared by annealing, 10 wt% PS doped PNIPAM particles at five different heating and cooling rates at temperatures ranging from 10 to 100°C. I_{tr} presented a hysteresis loops during heating–cooling cycles, which were explained by void closure and void reconstruction processes. The corresponding activation energies were measured during reversible film formation process. Void closure and void reconstruction models were introduced to produce the activation energies.

Keywords: Annealing rates; polystrene latex; PNIPAM hydrogels; reversible film formation.

1. INTRODUCTION

In the last two decades, it has been well established that hydrogels play an important role in living systems and are of broad interest for a large variety of industrial products [1, 2]. These gels can be regarded as intermediates between solids and liquids, a property that manifests itself in a rather complex mixture of the properties of these limiting states. Thermosensitive systems like poly(*N*-isopropylacrylamide) (PNIPAM), hydrogels have attracted much attention [3], because the viscoelastic characteristics can be easily controlled by changing the temperature. On the other hand, the bioadhesive properties of these materials point to possible applications as drug delivery systems, in pharmacentical applications.

Large size PNIPAM gels have the disadvantage that the swelling and shrinking processes occur on a rather long time-scale. Quick response to external stimuli, however, is a prerequisite for most potential applications. This difficulty can be

*To whom correspondence should be addressed. E-mail: pekcan@isikun.edu.tr

overcome by decreasing the size of PNIPAM particles to mesoscopic dimensions. Therefore, synthesis and characterisation of colloidal microgels has recently become quite popular [4, 5]. It has been understood that neutral colloidal PNIPAM particles with a diameter of some hundred nanometres have similar characteristics to their macroscopic counterparts, concerning the transition temperature and swelling capacity of the volume phase transition. Because of their fast kinetic response, microgels are good candidates to gain more insight into the physical nature of the volume phase transition [6–8]. It is well established from dynamic light scattering (DLS) and small-angle neutron scattering (SANS) that the swelling behaviour of macroscopic PNIPAM hydrogels depends on the amount of cross-linker introduced into the polymer network [9, 3]. In equilibrium conditions the network elasticity is balanced by the osmotic pressure of the system. The neutron scattering intensity is determined by a solid-like contribution from structural inhomogeneities of the gel matrix and a fluid-like component, which is attributed to local thermal fluctuations of the polymer chains. A growing number of cross-linking points increase the heterogeneity of the network structure. These internal parameters reduce the swelling capability of the macroscopic gel.

The term 'latex film' normally refers to a film formed from soft latex particles (T_g below room temperature) where the forces accompanying the evaporatian of water are sufficient to compress and deform the particles into transparent, void-free film [10]. However, latex films can also be obtained by compression moulding of a film of dried latex powder composed of relatively hard polymers such as polystyrene (PS) or poly(methyl methacrylate) (PMMA) that have T_g above room temperature. Hard latex particles remain essentially discrete and undeformed during drying. The mechanical properties of such films can be evolved after all solvent has evaporated by an annealing process that first leads to void closure and then interdiffusion of chains across particle–particle interfaces [11]. Film formation from soft and hard latex dispersions can occur in several stages. In both cases, the first stage corresponds to the wet initial state. Evaporation of solvent leads to the second stage in which the particles form a close packed array; here, if the particles are soft they are deformed to polyhedrons. Hard latex however stays undeformed at this stage. Annealing of soft particles causes diffusion across particle–particle boundaries which leads the film to form a homogeneous continuous material. In the annealing of a hard latex system, however, deformation of particles first leads to void closure [10, 12] and then after the voids disappear diffusion across particle–particle boundaries starts, i.e. the mechanical properties of hard latex films evolve during annealing, after all solvent has evaporated and all voids have disappeared.

Transmission electron microscopy (TEM) has been the most common technique used to investigate the structure of dried films [13, 14]. Pattern of hexagons, consistent with face centered cubic packing, are usually observed in highly ordered films. When these films are annealed, complete disappearance of structure is sometimes observed, which is consistent with extensive polymer interdiffusion. Freeze fracture TEM (FFTEM) has been used to study the strueture of dried latex

Downloaded by [The University of British Columbia] at 11:08 10 December 2014

Downloaded by [The University of British Columbia] at 11:08 10 December 2014

films [15, 16]. Small-angle neutron scattering (SANS) has been used to study latex film formation at the molecular level. Extensive studies using SANS have been performed by Sperling and coworkers [17] on compression moulded PS films. Direct-nonradiative energy transfer (DET) method has been employed to investigate the film formation processes from dye-labeled hard [18] and soft [19, 20] polymeric particles. The steady state fluorescence (SSF) technique combined with DET was used to examine healing and interdiffusion processes in dye-labeled hard latex systems [21–25]. Recently, UV-Visible technique was used to study film formation from PS and PMMA films [26–30], where the transmitted light intensity was monitored during film formation process.

In our previous study, we examined the film formation from nano-sized poly(*N*-isopropylacrylamide) (PNIPAM) microgel particles during heating–cooling cycles at various rates by using UV-visible technique [31]. A reversible film formation behavior from this soft particle system was observed during heating–cooling cycles. In the current work, we tried to understand the effect of hard PS latex on the reversible film formation behavior of a soft particle system. For this purpose, film formation from 10 wt% PS doped PNIPAM particles was studied by using photon transmission technique. Films were prepared by mixing PS and PNIPAM particles at five different heating and cooling temperature ranging from 10 to 100°C. The transmitted light intensity, I_{tr} was monitored during heating–cooling cycles. The increase and decrease in I_{tr} during these cycles were explained by void closure and void reconstruction processes. The corresponding activation energies were measured.

2. EXPERIMENTAL

2.1. PS latex particles

Pyrene labeled polystrene particles were produced *via* surfactant free emulsion polymerization process. The polymerization was carried out in a four-neck glass reactor equipped with a glass paddle agitation, condenser and nirogen inlet. The agitation rate was 300 rpm and the polymerization temperature was controlled at 70°C. Water (100 ml) and styrene (5 g) and 0.011 g of fluorescent 1-pyrenylmethylmethacrylate (PolyFluor 394) were first mixed in the polymerization reactor and when the temperature was constant (at 70°C), potassium peroxodisulfate (KPS) initiator (0.2 g) dissolved in a small amount of water (2 ml) was introduced in order to induce styrene polymerization. The polymerization was conducted for 18 h [32]. The synthesized latex particles are fairly monodisperse, having all very similar mean diameters (900 nm).

2.2. PNIPAM hydrogels

Fluorescent poly(*N*-isopropylacrylamide) microgel particles were synthesized *via* a precipitation polymerization process. *N*-isopropylacrylamide (NIPAM) from Ko-

dak was purified using a 60/40 (v/v) hexane and toluene mixture. Methylene bisacrylamide (MBA) from Aldrich was used as cross-linker monomer and was used as-received. Fluorescent monomer 1-pyrenylmethylmethacrylate (PolyFluor™ 394) was from Polysciences, Inc. and was used as-received. The polymerization was performed using (1.2 g) NIPAM, (0.059 g) MBA and (0.018 g) KPS as initiator. The recipe established by Menuier *et al*. [33, 34] was slightly modified by introducing an appropriate fluorescent (0.0054 g 1-pyrenylmethylmethacrylate) material. All the reactants were first solubilized in water and introduced into the polymerization reactor. The polymerization was conducted (in 50 ml deionised water) under nitrogen atmosphere and at 70°C. The polymerization reaction was carried out in a 100 ml four-necked glass reactor equipped with a glass anchor-type agitation (200 rpm), condenser and nitrogen inlet. The polymerization reaction was conducted for 16 h. The final conversion was gravimetrically determined and found to be 98.5%. The mean diameter of synthesized PNIPAM particles is 320 nm and the T_g of these cross-linked gels is 194°C.

2.3. PS doped PNIPAM films

Five different films were prepared from the mixture of PNIPAM and PS dispersion of particles by placing the same number of drops on a glass plates with the size of 0.8×2.5 cm^2 and allowing the water to evaporate. PS content in these films was chosen as 10 wt%. These samples were separately heated and cooled at five different rates (18.0, 9.4, 4.7, 3.1, 2.3°C/min) at temperatures ranging from 10 to 100°C. The temperature was maintained within 0.1°C for 20–40°C and 1°C for 40–100°C during annealing. Figure 1(a) and 1(b) present AFM images of 10 wt% PS particles doped PNIPAM film, before and after annealing, respectively.

2.4. Optical measurements

Photon transmission experiments were carried out using model DU 530 Life Science UV-Visible (UVV) spectrometer from Beckman. The transmittances of the films were detected at 400 nm. A glass plate was used as a standard for all UVV experiments. *In situ* measurements were carried out at different heating and cooling rates. AFM images were taken by using SPM-9500-J3 Shimadzu scanning probe microscopy.

3. VOID CLOSURE

Particle deformation and void closure between particles can be induced by shearing stress, which is generated by the surface tension of the polymer, i.e. polymer–air interfacial. The void closure kinetics can determine the time for optical clarity and film formation [35]. An expression to relate the shrinkage of spherical void of radius r, to the viscosity of surrounding medium, η, was derived and given by the

Downloaded by [The University of British Columbia] at 11:08 10 December 2014

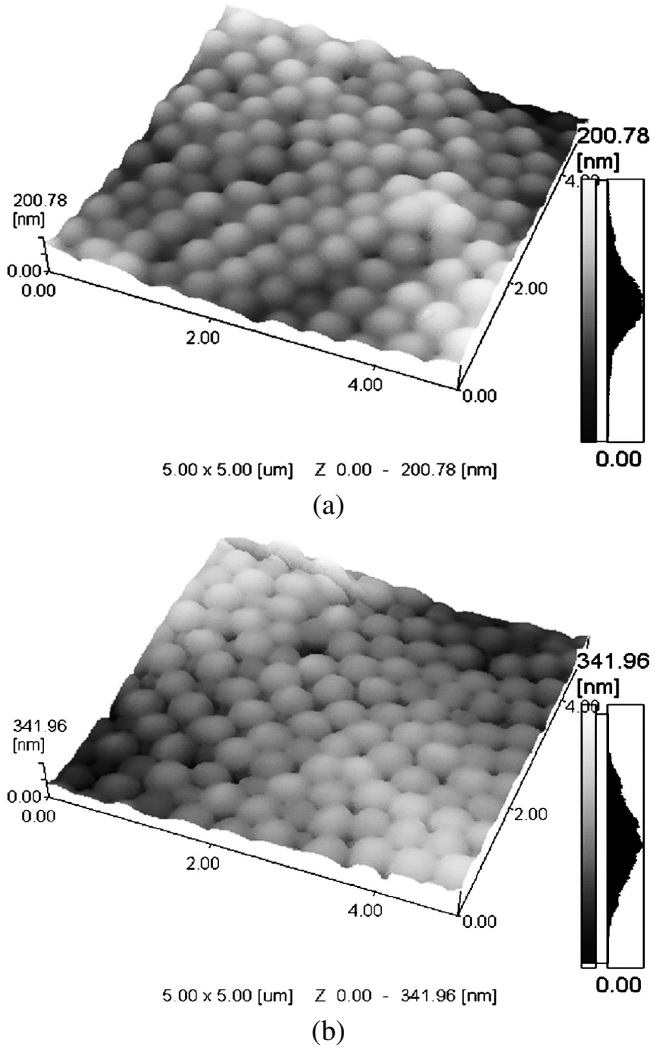


Figure 1. AFM images of the PNIPAM film doped with 10 wt% PS; (a) before void closure; (b) after void reconstruction.

following relation [36].

$$\frac{\mathrm{d}r}{\mathrm{d}t} = -\frac{\gamma}{2\eta}\left(\frac{1}{\rho(r)}\right), \tag{1}$$

where γ is the surface energy, t is time and $\rho(r)$ is the relative density. It has to be noted that here surface energy causes a decrease in void size and the term $\rho(r)$ varies with the microstructural characteristics of the material, such as the number of voids, the initial particle size and packing. Here $\rho(r)$ can be defined as a volume ratio of polymeric material to voids where, as r goes to zero, $\rho(r)$ increases; however, for large r values, $\rho(r)$ decreases. Equation (1) is quite similar to one which was

Downloaded by [The University of British Columbia] at 11:08 10 December 2014

used to explain the time dependence of the minimum film formation temperature during latex film formation [37, 38]. If the viscosity is constant in time, integration of equation (1) gives the relation as

$$t = -\frac{2\eta}{\gamma}\int_{r_0}^{r}\rho(r)\,\mathrm{d}r, \tag{2}$$

where r_0 is the initial void radius at time $t = 0$.

The dependence of the viscosity of polymer melt on temperature is affected by the overcoming of the forces of macromolecular interaction, which enables the segments of polymer chain to jump over from one equilibration position to another. This process happens at temperatures at which free volume becomes large enough and is connected with the overcoming of the potential barrier. The height of this barrier can be characterized by free energy of activation, ΔG, during viscous flow. Frenkel–Eyring [39] theory produces the following relation for the temperature dependence of viscosity:

$$\eta = \frac{N_0 h}{V}\exp\left(\frac{\Delta G}{kT}\right), \tag{3}$$

where N_0 is Avogadro's number, h is Planck's constant, V is molar volume and k is Boltzmann's constant. It is known that $\Delta G = \Delta H - T\Delta S$; then equation (3) can be written as

$$\eta = A\exp\left(\frac{\Delta H}{kT}\right), \tag{4}$$

where $\Delta H$is the activation energy of viscous flow, i.e. the amount of heat which must be given to one mole of material to create the act of a jump during viscous flow. ΔS is the entropy of activation of viscous flow. Since PNIPAM particles used in this study are cross-linked and have a $T_g = 194°C$, ΔS does not change with temperature. Therefore, A presents a constant for the related parameters including ΔS which does not depend on temperature. Combining equations (2) and (4) the following useful equation is obtained

$$t = -\frac{2A}{\gamma}\exp\left(\frac{\Delta H}{kT}\right)\int_{r_0}^{r}\rho(r)\,\mathrm{d}r. \tag{5}$$

Equation (5) can be employed by assuming that the interparticle voids are equal in size and that the number of voids stays constant during film formation (i.e. $\rho(r) \propto r^{-3}$). Then integration of equation (5) gives the relation

$$t = \frac{2AC}{\gamma}\exp\left(\frac{\Delta H}{kT}\right)\left(\frac{1}{r^2} - \frac{1}{r_0^2}\right), \tag{6}$$

where C is a constant related to relative density $\rho(r)$.

Downloaded by [The University of British Columbia] at 11:08 10 December 2014

4. RESULTS AND DISCUSSION

Transmitted photon intensities, I_{tr} from pure PNIPAM films *vs* annealing temperature in various heating and cooling rates are presented in Fig. 2. It is seen in Fig. 2. that films became more transparent as they annealed at higher temperatures by pre-

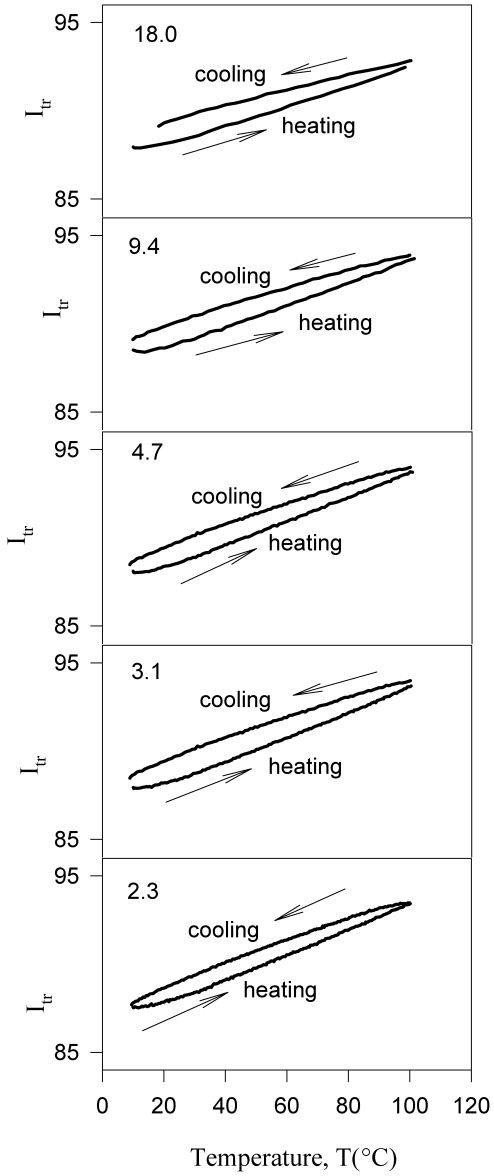


Figure 2. Transmitted light intensity, I_{tr} *versus* temperature curves for pure PNIPAM films in various heating–cooling rates. Arrows present heating and cooling cycles. Numbers on each figure indicate the rates in °C/min.

Downloaded by [The University of British Columbia] at 11:08 10 December 2014

Downloaded by [The University of British Columbia] at 11:08 10 December 2014

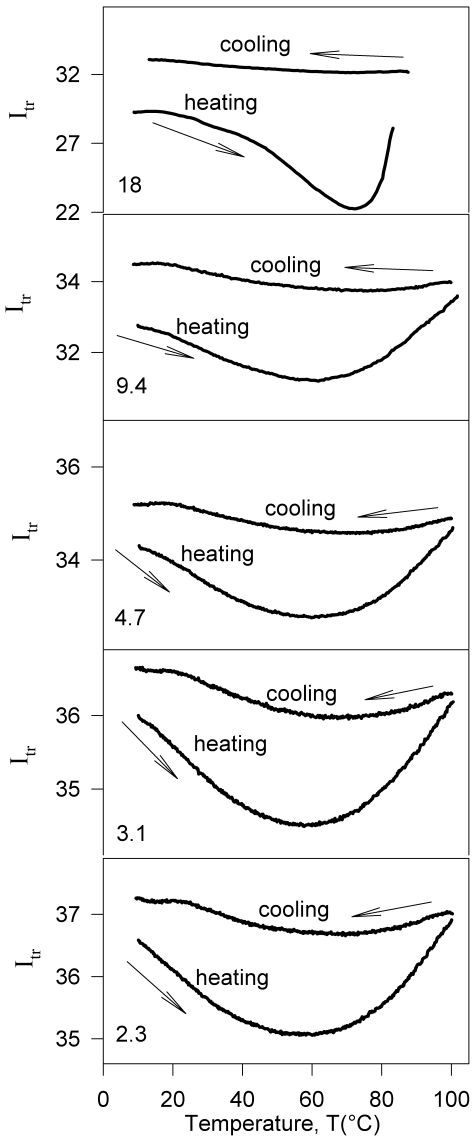


Figure 3. Transmitted light intensity, I_{tr} *versus* temperature, T curves for 10 wt% PS doped PNIPAM films in various heating–cooling rates. Arrows present cooling and heating cycles. Numbers on each figure indicate the rates in °C/min.

senting hysteresis loops at all cooling–heating rates. Figure 3 presents transmitted light intensity, I_{tr}, *versus* temperature, T, curves of 10% PS content PNIPAM films in various cooling–heating rates. Similarly, all curves in Fig. 3 present hysteresis by predicting a reversible film formation process. Except pure PNIPAM films, all other films show a minimum in heating and cooling cycles. It is seen in Fig. 3 that inclusion of PS into the PNIPAM lattice strongly decreases the transmitted light

intensity. Hysteresis loops of I_{tr} upon heating and cooling present different areas. Areas under the hysteresis curves for different heating–cooling rates are plotted in Fig. 4. On the other hand, the maxima of transmitted light intensity, $(I_{tr})_{max}$, for cooling curves *versus* heating–cooling rates are plotted in Fig. 5, where it is seen that $(I_{tr})_{max}$ has dropped to lower values at higher rates. Presumably, larger areas for heating–cooling cycles may correspond to slower relaxation of the PS–PNIPAM system during film formation process. In the pure PNIPAM system, no such area variation is observed. Doping the PNIPAM hydrogels with PS latex causes such relaxation process. In other words, inclusion of 10% PS into the PNIPAM delays the film formation process, especially at high heating–cooling rates. Decrease in $(I_{tr})_{max}$ at high heating–cooling rates however predicts the difficulties of film formation process from PS doped PNIPAM system.

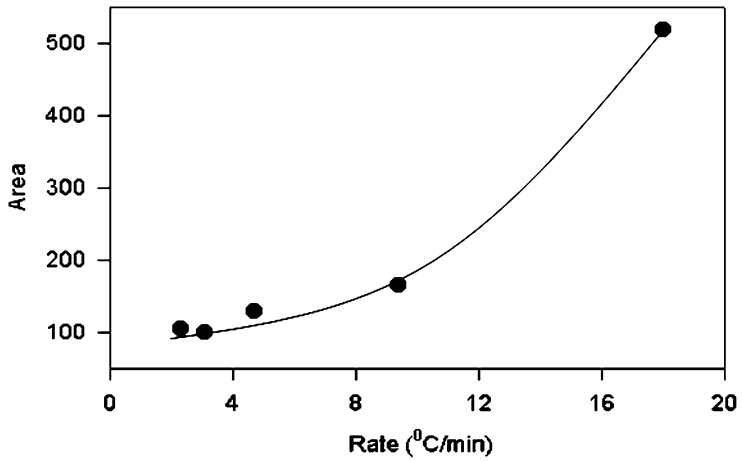


Figure 4. Plot of the areas under hysteresis curves *versus* heating–cooling rates.

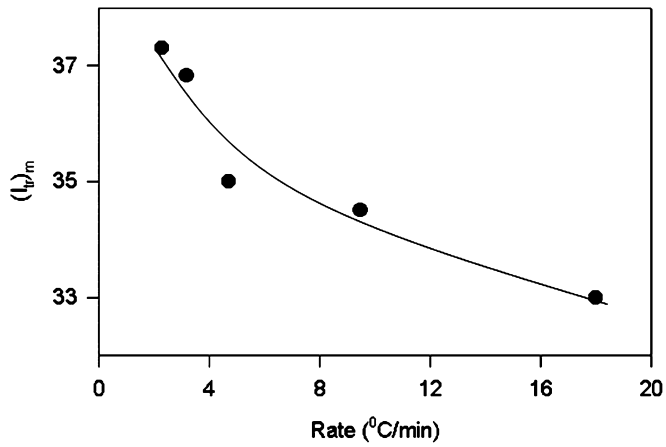


Figure 5. Plot of $(I_{tr})_{max}$ *versus* heating–cooling rates.

Downloaded by [The University of British Columbia] at 11:08 10 December 2014

Downloaded by [The University of British Columbia] at 11:08 10 December 2014

In order to quantify the heating and cooling curves presented in Fig. 3, the void closure model can be applied, where decrease in void size (r) causes an increase in $I_{\rm tr}/(I_{\rm tr})_{\rm max}$ ratios and *vice versa*. If the assumption is made that $I_{\rm tr}/(I_{\rm tr})_{\rm max}$ ratio is inversely proportional to the 6th power of the void radius, r, then equation (6) can be written as

$$t = \frac{2AC}{\gamma} \exp\left(\frac{\Delta H}{kT}\right)\left(\frac{I_{\rm tr}}{(I_{\rm tr})_{\rm max}}\right)^{1/3}. \tag{7}$$

Here, r_0^{-2} is omitted from the relation since it is very small compared to r^{-2} values after the void closure processes has started. Equation (7) can be solved for $I_{\rm tr}/(I_{\rm tr})_{\rm max}$

$$I_{\rm tr}(T) = S(t) \exp\left(-\frac{3\Delta H}{kT}\right), \tag{8}$$

where $S(t) = (yt/(2AC))^3$ and $I_{\rm tr} = I_{\rm tr}/(I_{\rm tr})_{\rm max}$. For a given time, the logarithmic form of equation (8) can be written as follows

$$\ln I_{\rm tr}(T) = \ln S(t) - \left(\frac{3\Delta H}{k_{\rm B}T}\right). \tag{9}$$

Equation (9) can now be used to produce ΔH activation energies. In Fig. 6(a) and 6(b), $\ln I_{\rm tr}$ *versus* T^{-1} plots and their fits to equation (9) are presented for heating and cooling processes, respectively. Here, void closure (ΔH_1 and ΔH_2) and void reconstruction (ΔH_{11} and ΔH_{22}) activation energies were produced from heating and cooling curves, respectively. The produced ΔH activation energies are plotted *vs* rates for the heating process in Fig. 7. It is seen that two different activation energies were observed for the heating processes. In other words, void closure in PS doped PNIPAM films is a two-step process. At first,

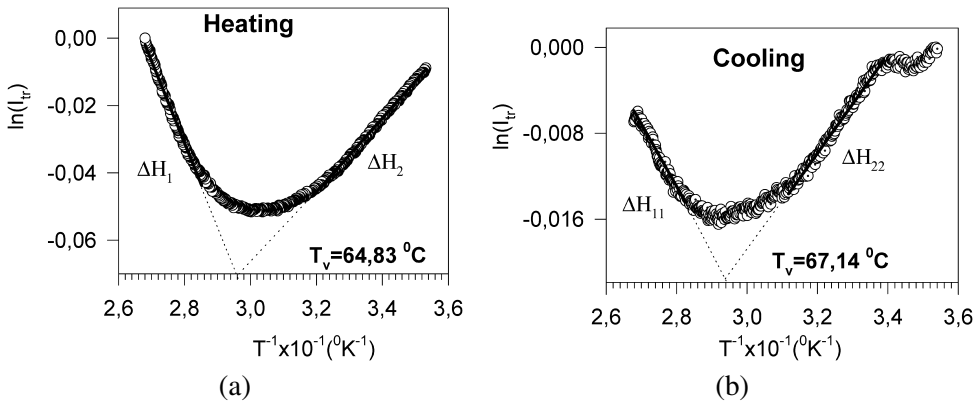


Figure 6. (a) Plots of $\ln I_{\rm tr}$ *versus* T^{-1} curves and their fits to equation (9) for heating process. The slopes of straight lines produced void closure activation energies (ΔH_1 and ΔH_2); (b) plots of $\ln I_{\rm tr}$ *versus* T^{-1} curves and their fits to equation (9) for cooling process. The slopes of straight lines produced void reconstruction activation energies (ΔH_{11} and ΔH_{22}).

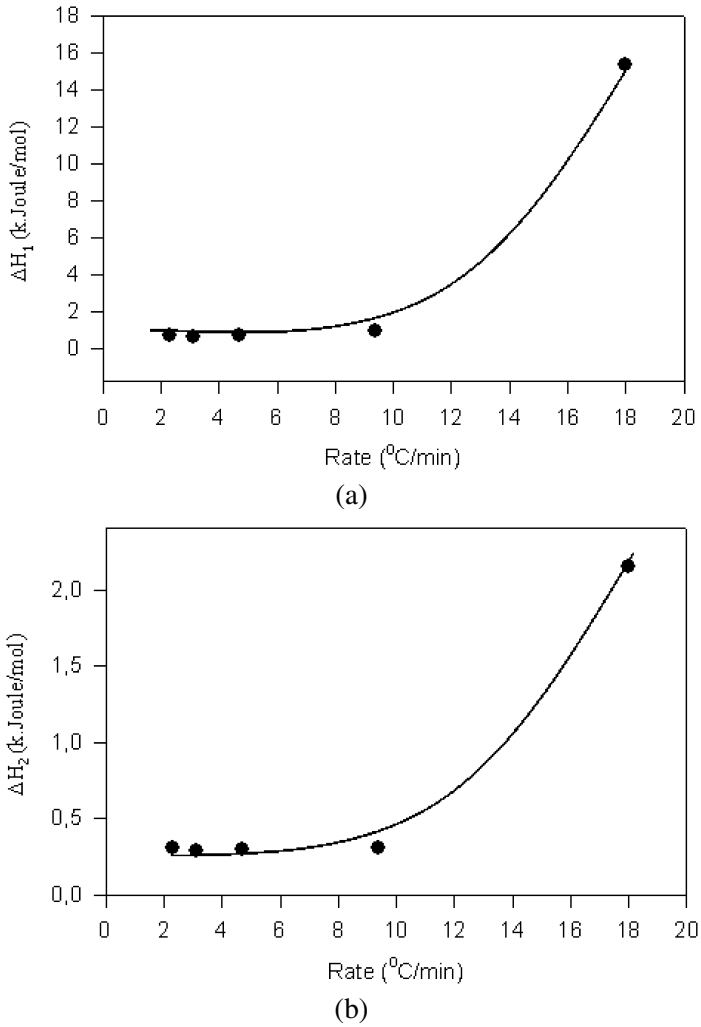


Figure 7. Plots of void closure activation energies (a) ΔH_1 and (b) ΔH_2 against heating rates.

the system takes an energy to accomplish phase separation, and then releases its energy to form a homogenous film during heating. Figure 7(a) and 7(b) both predict that the PS–PNIPAM system requires higher energies at higher rates to accomplish the void closure process. In other words, a slow response of the system during void closure process requires larger energies. Similarly during cooling, the PS–PNIPAM system takes and gives back its energy for reversible void reconstruction process, ending the film with voids again. It is seen in Table 1 that ΔH energies scattered as rate is increased, indicating that reconstruction processes require unpredictable energies in order to be completed, and/or these scattered data orginated from the low slopes of the reconstruction curves. Here we have to note that I_{tr} decreases during phase separation and then increases during

Downloaded by [The University of British Columbia] at 11:08 10 December 2014

Table 1.
Void reconstruction activation energies (ΔH_{11} and ΔH_{22}) during cooling process

Rate (°C/min)	18.0	9.4	4.7	3.1	2.3
ΔH_{11} (kJ/mol)	0.0448	0.1359	0.1738	0.1204	0.0991
ΔH_{22} (kJ/mol)	0.1242	0.1453	0.1132	0.0657	0.1273
T_v (°C)	78.12	69.46	74.22	71.83	67.14

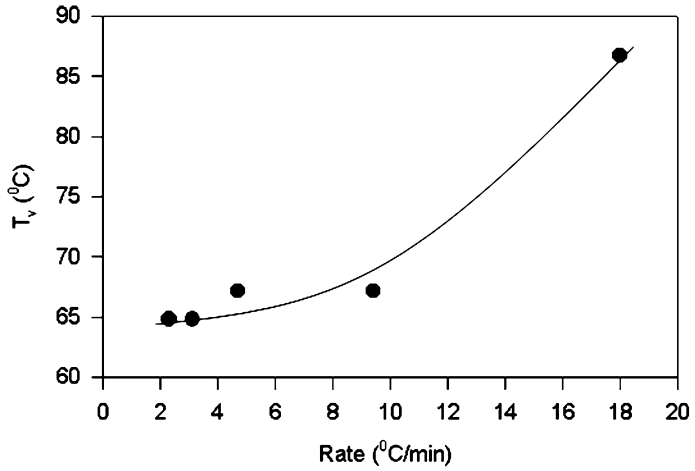


Figure 8. Plots of intercept temperature, T_v, shown in Fig. 6 *versus* heating rates.

homogeneus film formation during heating, dividing the void closure into a two-step process. During cooling, however, these processes are reversed to complete the void reconstruction process.

Careful analysis of Fig. 6 shows that increasing rate causes a shift of the intercept (T_v) of the straight lines to higher temperatures. The observed temperatures, T_v, are plotted *versus* rate in Fig. 8 for the heating process. Intercept temperature, T_v, increased as rate increased, predicting that a higher temperature is required for film formation from doped films at higher rates. This result is consistent with high energy and slow relaxation requirements at higher heating rates.

5. CONCLUSION

Doping of the hydrophilic matrix (PNIPAM) with hydrophobic particles (PS) caused two-step void closure and reconstruction processes, unlike the behaviour of a pure PNIPAM system, in which single-step processes were observed [31]. In both cases, hysteresis occurs, but in the doped film the hysteresis cycles go through the minima. Most probably, this two-step phenomenon in PS doped PNIPAM system

Downloaded by [The University of British Columbia] at 11:08 10 December 2014

occurs due to the phase separation process, which originates from the hydrophobic–hydrophylic nature of the system under consideration.

REFERENCES

1. Y. Hirokawa and T. Tanaka, Volume phase-transition in a nonionic gel, *J. Chem. Phys.* **81**, 6379–6380 (1984).
2. M. Shibayama, Spatial inhomogeneity and dynamic fluctuations of polymer gels, *Macromol. Chem. Phys.* **199**, 1–30 (1998).
3. M. Shibayama, T. Tanaka and C. C. Han, Small-angle neutron-scattering study on poly(*N*-isopropyl acrylamide) gels near their volume-phase transition-temperature, *J. Chem. Phys.* **97**, 6829–6841 (1992).
4. K. Kratz and W. Eimer, Swelling properties of colloidal poly(*N*-isopropylacrylamide) microgels in solution, *Ber. Bunsenges Phys. Chem.* **102**, 848–854 (1998).
5. K. Kratz, T. Hellweg and W. Eimer, Effect of connectivity and charge density on the swelling and local structural and dynamic properties of colloidal PNIPAM microgels, *Ber. Bunsenges Phys. Chem.* **102**, 1603–1608 (1998).
6. K. S. Oh, J. S. Oh, H. S. Choi and Y. C. Bae, Effect of cross-linking density on swelling behavior of NIPA gel particles, *Macromolecules* **31**, 7328–7335 (1998).
7. N. Dingenouts, C. Nordhausen and M. Ballauff, The volume transition in thermosensitive micronetworks as observed by small-angle X-ray scattering, *Ber. Bunsenges Phys. Chem.* **102**, 1594–1596 (1998).
8. R. Pelton, Temperature-sensitive aqueous microgels, *Adv. Colloid. Interf. Sci.* **85**, 1–33 (2000).
9. E. S. Matsuo and T. Tanaka, Kinetics of discontinuous volume phase-transition of gels, *J. Chem. Phys.* **89**, 1695–1703 (1988).
10. P. R. Speny, B. S. Snyder, M. L. O'Dowd and P. M. Lesko, The effect of environmental conditions on latex film formation, *Langmuir* **10**, 2619–2628 (1994).
11. S. Mazur, Coalescence of polymer particle, in: *Polymer Powder Processing*, N. Rosenweig (Ed.). John Wiley, New York, USA (1995).
12. J. K. Mackenzie and R. Shutlewort, A phenomenological theory of sintering, *Proc. Phys. Soc.* **62**, 838 (1946).
13. J. W. Vanderhoof, Mechanism of film formation of latices, *Chem. Proc. Engng.* **51**, 89 (1970).
14. G. Kanig and H. Neff, New contrast method for electron-microscopic study of acid and ester group containing polymer systems, *Colloid Polym. Sci.* **253**, 29–31 (1975).
15. Y. Wang, A. Kats, D. Juhue, M. A. Winnik, R. R. Shivers and C. J. Dinsdale, Freeze-fracture studies of latex films formed in the absence and presence of surfactant, *Langmuir* **8**, 1435–1442 (1992).
16. B. J. Roulstone, M. C. Wilkinson, J. Hearn and A. J. Wilson, Studies on polymer latex films. 1. A study of latex film morphology, *Polym. Int.* **24**, 87–94 (1991).
17. K. D. Kim, L. H. Sperling and A. Klein, Characterization of film formation from direct mini-emulsified polystyrene latex-particles *via* SANS, *Macromolecules* **26**, 4624–4631 (1993).
18. Ö. Pekcan, M. A. Winnik and M. D. Croucher, Fluorescence studies of polymer colloids. 25. Fluorescence studies of coalescence and film formation in poly(methylmethacrylate) nonaqueous dispersion particles, *Macromolecules* **23**, 2673–2678 (1990).
19. Y. Wang, C. L. Zhao and M. A. Winnik, Molecular-diffusion and latex film formation – an analysis of direct nonradiative energy-transfer experiments, *J. Chem. Phys.* **95**, 2143–2153 (1991).
20. Y. Wang and M. A. Winnik, Energy-transfer study of polymer diffusion in melt-pressed films of poly(methyl methacrylate), *Macromolecules* **26**, 3147–3150 (1993).

Downloaded by [The University of British Columbia] at 11:08 10 December 2014

21. Ö. Pekcan and M. Canpolat, Direct fluorescence technique to study evolution in transparency and crossing density at polymer–polymer interface during film formation from high-T latex particles, *J. Appl. Polym. Sci*. **59**, 277–285 (1996).
22. Ö. Pekcan, M. Canpolat and A. Göçmen, Variation in optical-density during latex film formation — interdiffusion of fluorescence-labeled polymers, *Polymers* **34**, 3319–3321 (1993).
23. M. Canpolat and Ö. Pekcan, Photon diffusion study in films formed from high-T latex-particles, *Polymer* **36**, 4433–4438 (1995).
24. Ö. Pekcan, Interdiffusion during latex film formation, *Trends Polym. Sci.* **5**, 177–180 (1994).
25. M. Canpolat and Ö. Pekcan, Healing and photon diffusion during sintering of high-T latex particles, *J. Polym. Sci. B, Polym. Phys.* **34**, 691–698 (1996).
26. Ö. Pekcan, E. Arda, K. Kesenci and E. Pişkin, Photon transmission technique for studying film formation from polystyrene latexes prepared by dispersion polymerization using various steric stabilizers, *J. Appl. Polym. Sci.* **68**, 1257–1267 (1998).
27. E. Arda, V. Bulmuş, E. Pişkin and Ö. Pekcan, Molecular weight effect on latex film formation from polystyrene particles: a photon transmission study, *J. Coll. Int. Sci.* **213**, 160–168 (1999).
28. Ö. Pekcan and E. Arda, Molecular weight dependent changes with time during latex film formation: a photon transmission study, *Polym. Int.* **47**, 231–236 (1998).
29. Ö. Pekcan and E. Arda, Effect of molecular weight on latex film formation: a photon transmission study, *J. Appl. Polym. Sci.* **70**, 339–351 (1998).
30. Ö. Pekcan and E. Arda, Void closure and interdiffusion in latex film formation by photon transmission and fluorescence methods, *Colloids and Surfaces A* **153**, 537–549 (1999).
31. S. Ugur, A. Elaissari, O. Yargi and O. Pekcan, Reversible film formation from nano-sized PNIPAM particles below glass transition, *Coll. Polym. Sci.* **285**, 423–430 (2007).
32. Ş. Uğur, A. Elaissari and Ö. Pekcan, Void closure and interdiffusion processes during latex film formation from surfactant-free polystyrene particles: a fluorescence study, *J. Coll. Interface Sci.* **263**, 674–683 (2003).
33. F. Meunier, A. Elaissari and C. Pichot, Preparation and characterization of cationic poly(N-isopropylacrylamide) copolymer latexes, *Polym. Adv. Tech*. **6**, 489–496 (1995).
34. F. Meunier and A. Elaissari, Poly(N-isopropylacrylamide)-based particles: preparation and colloidal characterization, *Surfactant Science Series* **115**, 117–144 (2003).
35. J. L. Keddie, P. Meredith, R. A. L. Jones and A. M. Ronald, Rate-limiting steps in the film formation of water-borne acrylic lattices as elucidated with ellipsometry and environmental-SEM, *Proc. ACS 210, 76-PSME*, Part 2 (1995).
36. P. R. Sperry, B. S. Snyder, M. L. O'Dowd and P. M. Lesko, Role of water in particle deformation and compaction in latex film formation, *Langmuir* **10**, 2619–2628 (1994).
37. J. K. Mackenzie and R. Shutlewort, A phenomenological theory of sintering, *Proc. Phys. Soc.* **62**, 838 (1949).
38. G. B. McKenna, in: *Comprehensive Polymer Science*, C. Booth and C. Price (Eds), Vol. 2. Pergamon Press, Oxford, UK (1989).
39. A. Tager, *Physical Chemistry of Polymers*. MIR Publisher, Moscow, USSR (1978).

Downloaded by [The University of British Columbia] at 11:08 10 December 2014